Practical Hybrid Beamforming Schemes in Massive MIMO 5G NR Systems

Xiaoguang Zhao, Elena Lukashova, Florian Kaltenberger, Sebastian Wagner
EURECOM, TCL
Campus SophiaTech, 450 Route des Chappes, 06410 Biot, France
Email: (xiaoguang.zhao, elena.lukashova)@eurecom.fr

***Abstract*—Massive MIMO systems in millimiter-wave band rely on beamforming techniques to focus transmit energy in a specific direction. Hybrid beamforming, which typically includes analog wideband and digital subband components, is designed as a compromise between affordable but low precision fully analog schemes and energy-consuming, expensive fully digital approaches. In this paper, we apply a practical approach to hybrid beamforming for Single User 5G Massive Multiple-Input-Multiple-Output (MIMO) Systems. In the 5G New Radio (NR) simulator, we implement and experimentally validate dual-stage hybrid beamforming approaches based on Singular Value Decomposition of the channel matrix and Zero Forcing, while fully digital scheme is taken as a baseline. We quantify gain offered by partially and fully connected structures, various number of Radio Frequency chains and transmit antennas, in terms of throughput and Block Error Rate. Varying the number of phase shifters, we investigate the performance-complexity trade-off for resolution of the phase shifters. To adequately reflect propagation environment, the simulations were run with Clustered Delay Line CDL-A channel model with angle scaling.**

I. Introduction

Increase in uniform throughput can be accomplished in three ways: bandwidth extension, deploying multiple antennas at the base stations and user equipment (UE), and network densification [1]. The millimeter-wave (mmWave) band for the new generation of wireless communications standards, 5G New Radio (NR), was conceived to solve bandwidth limitations, which are common for older wireless communications systems in microwaves bands. As a second key point, a short wavelength enables the use of large antennas arrays packed into small form-factors [2], making it possible to implement large-scale massive Multiple-Input-Multiple-Output (MIMO) antenna arrays. Massive MIMO systems in mmWave band thus deliver throughput, spectral efficiency, and network capacity which significantly overcome those of previous wireless standards [3], [4]. However, these advantages come at cost of high propagation loss and challenging mobility support. To cope with cluttered propagation environment and restricted link budget, mmWave band transmission relies on directional transmissions and receptions.

Thanks to the large number of antenna elements at the base station, Massive MIMO systems can be used to serve spatially separated users by forming multiple beams and focusing transmitted energy in specific directions. The beamforming consists in selecting a precoding matrix (at the transmitter) and a combiner matrix (at the receiver) based on some Channel State Information (CSI). CSI can be explicit (quantized channel coefficients, correlation matrix), implicit (quantized codebook-based precoding) [5], or obtained through channel reciprocity in Time Division Duplex systems.

Beamforming techniques can be classified as analog, digital and hybrid. Analog beamforming can be used to control the phase of the transmitted signal, which is usually implemented with phase shifters. Digital beamforming has the flexibility of controlling the amplitude and phase of the signal, requiring dedicated baseband and radio frequency (RF) chains for the signal processing. However, the fully digital beamforming is not practical for the mmWave band, since it requires one distinct RF chain per antenna. RF chains include analog-to-digital converters (ADCs) and digital-to-analog converters (DACs), as well as power and low noise amplifiers, are rather expensive and power-consuming for wideband mmWave systems.

Hybrid beamforming was first introduced in [6], and is designed as a compromise between affordable but low precision analog schemes and energy-consuming, expensive fully digital approaches [7], [8]. This compromise is achieved by deploying fewer RF chains than transmit antennas, with the minimum number equal to the number of the data streams. To achieve the performance level of fully digital structures, the hybrid design requires twice or more RF chains N_{RF} than number of data streams N_s [9]. For practical implementations, hybrid algorithms can be configured with fully or partially connected antenna array structures, as well as with finite and infinite resolution phase shifters.

Hybrid precoding matrix can be seen as a product of analog $\mathbf{V}_{\text{RF}}$ and digital $\mathbf{V}_{\text{dig}}$ components. In practical systems, the analog part is wideband and is designed to capture long-term channel variations, whereas the digital part aims to compensate for the short-term channel fluctuations, and can vary between different subcarriers or subbands.

The optimal criterion for precoding matrices is the maximum user data rate. However, even in the presence of full instantaneous CSI at the transmitter, obtaining hybrid precoding and combining matrices is still challenging [10]. First, analog and digital precoding matrices are coupled, such that the objective function of the sum data rate is non-convex. Second, the analog beamformers have additional constraints that the amplitude of $v_{\text{RF}}(i,j)$ equals one, where $v_{\text{RF}}(i,j)$ is i and j are respectively rows and columns of $\mathbf{V}_{\text{RF}}$ [9]. Third,

for the finite-resolution phase shifters, the analog beamformer lies in a discrete set, which typically leads to NP-hard integer problems [11].

The majority of the existing works for Single-User MIMO (SU-MIMO) and Multi-User Multiple Input Single Output (MU-MISO) follows a two-stage approach. First, assuming the digital beamformer is a unitary matrix, the analog beamformer is optimized column by column by imposing the phase-only constraints on each antenna. Once the analog beamformer $\mathbf{V}_{\text{RF}}$ is known, the effective channel is defined as $\widetilde{\mathbf{H}}_{\text{eff}} = \mathbf{H}\mathbf{V}_{\text{RF}}$, where $\mathbf{H}$ is the channel matrix. The digital beamformer can now be solved using traditional digital beamforming algorithms, e.g. minimum mean squared error (MMSE), Zero-Forcing (ZF) [7], [9], [12], [13].

A few proposed approaches first design an optimal precoder $\mathbf{V}_{\text{opt}}$ for the fully digital structure. At second step, the optimal Orthogonal Matching Pursuit algorithm is applied to compute an equivalent hybrid matrix $\mathbf{V}_{\text{Hbf}} = \mathbf{V}_{\text{RF}}\mathbf{V}_{\text{dig}}$ by minimizing the mean squared error between $\mathbf{V}_{\text{opt}}$ and $\mathbf{V}_{\text{Hbf}}$ [10], [14].

Different hybrid beamforming structures were discussed in [15]. Following the fully connected principle (see Fig.1(a)), each RF chain is linked to N_{t} phase shifters (same as number of transmit antennas) which are then connected to each transmit antenna. The systems thus requires $N_{\text{PhS}} = N_{\text{t}}N_{\text{RF}}$ phase shifters in total. In contrast, in the partially connected scheme, illustrated in Fig.1(b) each RF chain is connected with $\frac{N_{\text{t}}}{N_{\text{RF}}}$ phase shifters, and each of them is connected to each transmit antenna. The total number of the phase shifters for partially connected schemes is thus reduced to $N_{\text{PhS}} = N_{\text{t}}$. Fully connected schemes are known to approach performance of digital structures, and outperform partially connected structures [12].

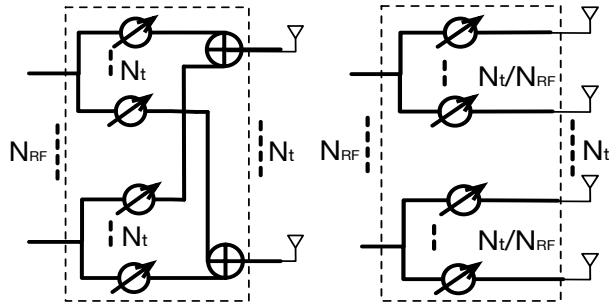

(a) Fully connected (b) Partially connected

Fig. 1. Fully connected and partially connected hybrid antenna array architectures

The majority of existing works are restricted to a simple frequency-flat propagation environment. For the practical evaluations and model validations, it is important to consider the hybrid beamforming schemes in mmWave wideband OFDM system with frequency selective channels. In addition, more complicated channel models are required to reflect antenna geometry. As defined in the 5G standards, Clustered Delay Line (CDL) channel model with angle scaling [16] can be used for link-level simulation for massive MIMO with beamforming.

Another hybrid approach is ZF beamforming, which, provided a large number of antennas at the transmitter, approaches performance of the optimal digital scheme [17] like Dirty Paper Coding [18].

In this paper, we consider the hybrid beamforming for SU-MIMO system with total power constraint, which means that the total power of the precoded signal for the duration of one symbol time remains the same after the precoding. Our hybrid beamforming algorithm can be applied for fully or partially connected antenna array structures based on finite or infinite resolution phase shifters. In hybrid beamforming scheme proposed by [12], the digital component is obtained on pre-subcarrier basis through a water-filling solution. In contrast with [12], we first use singular value decomposition (SVD) precoder without water-filling power allocation as the baseband digital precoder at the transmitter. Following this, a general total power scaling factor is applied to all the subcarriers to satisfy the total power constraint at the transmitter. We then compare SVD and ZF choice for the digital component for our hybrid beamforming matrix. The UE performs signal detection based on reduced complexity maximum-likelihood LLR metrics, developed by [19]. In scenarios with SVD beamforming, the detection is preceded by the SVD combining matrix.

We experimentally evaluate the performance of the hybrid and digital beamforming using MATLAB-based 5G NR link-level simulator. Instead of the stochastic cluster scattering channel model [10], we use CDL-A channel, which reflects real environments more realistically. The model is defined for the frequency range from 0.5 GHz to 100 GHz with a maximum bandwidth of 2 GHz. The performance of the hybrid and digital beamforming for massive MIMO is verified based throughput and Block Error Rate (BLER) performance metrics.

II. System Model

In practical massive MIMO systems, the number of antennas at the base station is significantly larger than that of antennas at the receiver. The UEs are usually equipped with four antennas or fewer. We consider a downlink transmission in OFDM Single-User massive MIMO system with hybrid beamforming at the gNB and fully digital combiner at the UE, as depicted in Fig.2.

The gNB equipped with N_{t} transmit antennas, N_{RF} RF chains and N_{s} data streams serves a single user with N_{r} receive antennas. At the base station, symbol $\mathbf{s}$ are multiplied with the low-dimensional digital precoder matrix $\mathbf{V}_{\text{dig}}$, and are then mapped onto 5G NR resource grid in frequency domain. The resulting signal undergoes orthogonal frequency-division multiplexing (OFDM) modulation. The time domain signal now gets precoded by analog precoder $\mathbf{V}_{\text{RF}}$, which is implemented with phase shifters. The received signal $\mathbf{y}[k]$ seen

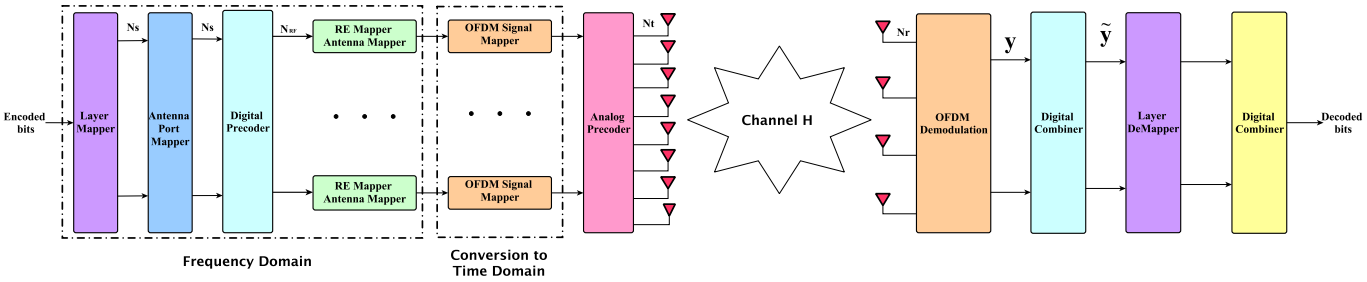

Fig. 2. Block diagram of a SU-MIMO system with hybrid transmitter and fully digital receiver

at the UE on the k-th $(k = 1, \ldots, K)$ subcarrier, can be written as

$$\mathbf{y}[k] = \mathbf{H}[k]\mathbf{V}_{\text{RF}}\mathbf{V}_{\text{dig}}[k]\mathbf{s}[k] + \mathbf{z}[k], \tag{1}$$

where $\mathbf{s}[k] \in \mathbb{C}^{N_s \times 1}$ is the signal after layer mapping, $\mathbf{V}_{\text{dig}}[k] \in \mathbb{C}^{N_{\text{RF}} \times N_s}$ and $\mathbf{V}_{\text{RF}} \in \mathbb{C}^{N_t \times N_{\text{RF}}}$ are digital and analog precoding matrices respectively, $\mathbf{H}[k] \in \mathbb{C}^{N_r \times N_t}$ is channel between the transmit and receive antennas, $\mathbf{z}[k] \sim \mathcal{CN}(0, \sigma^2\mathbf{I}_{N_r})$ is the additive complex white Gaussian noise, with zero mean and $\sigma^2\mathbf{I}_{N_r}$ covariance. To stress on the precoding transparency for the UE, we define an effective channel matrix $\mathbf{H}_{\text{eff}}$:

$$\mathbf{H}_{\text{eff}}[k] = \mathbf{H}[k]\mathbf{V}_{\text{RF}}\mathbf{V}_{\text{dig}}[k]. \tag{2}$$

Even though the UE does not know explicitly precoding matrices used by the base station, it acquires knowledge of the effective channel $\mathbf{H}_{\text{eff}}$ by performing channel estimation.

Perfect CSI knowledge between each transmit and receive antenna at the base station can be obtained through channel reciprocity with calibration via uplink training in Time-Division Duplex (TDD) system [20]. In this paper, CSI knowledge $\mathbf{H}[k]$ between each transmit antenna and receive antenna is assumed to be known in order to get the hybrid precoding matrix at the gNB side. While CSI knowledge is represented by effective channel matrix $\mathbf{H}_{\text{eff}}$ availability at the UE side. In such systems, the receiver uses the combining matrix to obtain the post-processed signal $\widetilde{\mathbf{y}}$:

$$\begin{aligned}\widetilde{\mathbf{y}}[k] &= \mathbf{W}^H[k]\mathbf{y}[k] &(3)\\ &= \mathbf{W}^H[k]\mathbf{H}_{\text{eff}}[k]\mathbf{s}[k] + \mathbf{W}^H[k]\mathbf{z}[k], &(4)\\ &= \underbrace{\mathbf{W}^H[k]\mathbf{H}[k]\mathbf{V}_{\text{RF}}\mathbf{V}_{\text{dig}}[k]}_{\mathbf{C}_{\text{eq}}[k]}\mathbf{s}[k] + \mathbf{W}^H[k]\mathbf{z}[k], &(5)\end{aligned}$$

where $\mathbf{W}[k]$ is the combining matrix at the k-th subcarrier and $\mathbf{C}_{\text{eq}}[k]$ denotes a product of the combining matrix, channel, digital and analog precoders.

Assuming Gaussian signaling, the achievable rate $r[k]$ at the k-th subcarrier in such system is

$$r[k] = \log_2\left|\mathbf{I}_{N_r} + \frac{\mathbf{C}_{\text{eq}}[k]\mathbf{C}_{\text{eq}}^H[k]}{\sigma^2}\right|, \tag{6}$$

where operand $|\mathbf{A}|$ denotes the determinant of the matrix $\mathbf{A}$.

The hybrid precoding optimization problem, aimed at maximizing the sum rate across K subcarriers of the served user, can be modeled as

$$\max_{\mathbf{V}_{\text{RF}}, \mathbf{V}_{\text{dig}}[k]} \ \frac{1}{K}\sum_{k=1}^{K} r[k], \tag{7a}$$

$$s.t. \ \sum_{k=1}^{K} \text{Tr}(\mathbf{V}_{\text{RF}}\mathbf{V}_{\text{dig}}[k]\mathbf{V}_{\text{dig}}^H[k]\mathbf{V}_{\text{RF}}^H) \le P, \tag{7b}$$

$$|\mathbf{V}_{\text{RF}}(i,j)| = 1. \tag{7c}$$

where P is the total transmit power, $\mathbf{V}_{\text{RF}}(i,j)$ is the (i,j)-th element of $\mathbf{V}_{\text{RF}}$, and operand $|a|$ denotes the amplitude of the scalar a.

III. Hybrid Precoder and Digital Combiner

The optimal hybrid beamforming design involves joint design of precoding and combining matrix. We focus on fully digital receiver, which may simplify the design of our matrices. Assuming optimal linear fully-digital combiner at the receiver, the combiner matrix will not affect the mutual information between $\mathbf{s}[k]$ and $\mathbf{y}[k]$. Thus, we could decouple the design of the precoder and the combiner into a dual-stage approach. First, we design the hybrid precoder $\mathbf{V}_{\text{Hbf}}$ at the base station, and, as the second step, a digital combiner is designed based on the derived hybrid precoder $\mathbf{V}_{\text{Hbf}}$.

Assuming we know the optimal combiner, the hybrid beamforming optimization problem can be developed as

$$\max_{\mathbf{V}_{\text{RF}}, \mathbf{V}_{\text{dig}}[k]} \ \frac{1}{K}\sum_{k=1}^{K} \widetilde{r}[k] \tag{8a}$$

$$s.t. \quad \sum_{k=1}^{K} \text{Tr}(\mathbf{V}_{\text{RF}}\mathbf{V}_{\text{dig}}[k]\mathbf{V}_{\text{dig}}^H[k]\mathbf{V}_{\text{RF}}^H) \le P \tag{8b}$$

$$|\mathbf{V}_{\text{RF}}(i,j)| = 1 \tag{8c}$$

where rate $\widetilde{r}[k] = \log_2\left|\mathbf{I}_{N_r} + \frac{\mathbf{H}[k]\mathbf{V}_{\text{Hbf}}[k]\mathbf{V}_{\text{Hbf}}^H[k]\mathbf{H}^H[k]}{\sigma^2}\right|$, and $\mathbf{V}_{\text{Hbf}}[k] = \mathbf{V}_{\text{RF}}\mathbf{V}_{\text{dig}}[k]$ is the equivalent hybrid precoding matrix.

A. Analog Precoding Design

The analog beamforming is based on Sohrabi's papers [9], [12]. Assuming the digital precoder at the transmitter is a unitary matrix, where $\mathbf{V}_{\text{dig}}[k]\mathbf{V}_{\text{dig}}^H[k] = \gamma^2\mathbf{I}$ and γ is the power scaling factor, the power constraint for the hybrid optimization

problem is automatically satisfied. The achievable rate at subcarrier k can be further reduced as:

$$\max_{\mathbf{V}_{\text{RF}},\mathbf{V}_{\text{dig}}[k]} \frac{1}{K}\sum_{k=1}^{K}\log_2\left|\mathbf{I}_{N_\text{r}}+\frac{\gamma^2\mathbf{V}_{\text{RF}}^H\mathbf{H}^H[k]\mathbf{H}[k]\mathbf{V}_{\text{RF}}}{\sigma^2}\right|, \quad (9a)$$

$$s.t. \quad |v_{\text{RF}}(i,j)|=1 \quad (9b)$$

Using Jensen's inequality, the uppper bound is

$$\frac{1}{K}\sum_{k=1}^{K}\tilde{r}[k]=\frac{1}{K}\sum_{k=1}^{K}\log_2\left|\mathbf{I}_{N_\text{r}}+\frac{\gamma^2\mathbf{V}_{\text{RF}}^H\mathbf{H}^H[k]\mathbf{H}[k]\mathbf{V}_{\text{RF}}}{\sigma^2}\right|, \quad (10)$$

$$\leq \log_2\left|\mathbf{I}_{N_\text{r}}+\frac{\gamma^2\mathbf{V}_{\text{RF}}^H\mathbf{H}_{\text{cov}}\mathbf{V}_{\text{RF}}}{\sigma^2}\right|, \quad (11)$$

where $\mathbf{H}_{\text{cov}}=\frac{1}{K}\sum_{k=1}^{K}\mathbf{H}^H[k]\mathbf{H}[k]$ is the average covariance channel matrix across all the subcarriers.

Since analog precoding is wideband, the optimization can be reduced to frequency-flat channel. The optimal analog beamformer algorithm was developed by Sohrabi in [9] and we provide it in details below. Analog precoder is common for SVD and ZF hybrid schemes.

Extracting the contribution of the m-th column $\mathbf{v}_{\text{RF}}^{(m)}$ of the $\mathbf{V}_{\text{RF}}$, the objective function of the analog precoder design can be written as

$$\begin{aligned}&\log_2\left|\mathbf{I}_{N_\text{r}}+\frac{\gamma^2\mathbf{V}_{\text{RF}}^H\mathbf{H}_{\text{cov}}\mathbf{V}_{\text{RF}}}{\sigma^2}\right|\\ &=\log_2|\mathbf{C}_m|+\log_2\left|1+\frac{\gamma^2}{\sigma^2}{\mathbf{v}_{\text{RF}}^{(m)}}^H\mathbf{G}_m\mathbf{v}_{\text{RF}}^{(m)}\right|,\end{aligned} \quad (12)$$

where $\mathbf{C}_\text{m}=\mathbf{I}+\frac{\gamma^2}{\sigma^2}\left(\bar{\mathbf{V}}_{\text{RF}}^{(m)}\right)^H\mathbf{H}_{\text{cov}}\bar{\mathbf{V}}_{\text{RF}}^{(m)}$ and $\mathbf{G}_\text{m}=\mathbf{H}_{\text{cov}}-\frac{\gamma^2}{\sigma^2}\mathbf{H}_{\text{cov}}\bar{\mathbf{V}}_{\text{RF}}^{(m)}\mathbf{C}_m^{-1}(\bar{\mathbf{V}}_{\text{RF}}^{(m)})^H$, $\bar{\mathbf{V}}_{\text{RF}}^{(m)}$ is the sub-matrix of $\mathbf{V}_{\text{RF}}$ with m-th column removed.

Components $\mathbf{C}_\text{m}$ and $\mathbf{G}_\text{m}$ are independent of $\mathbf{v}_{\text{RF}}^{(m)}$. Assuming all the elements of the $\mathbf{v}_{\text{RF}}^{(m)}$ are known except for the n-th element v_{mn}, we can write

$${\mathbf{v}_{\text{RF}}^{(m)}}^H\mathbf{G}_\text{m}\mathbf{v}_{\text{RF}}^{(m)}=\varsigma_\text{mn}+2\Re\left\{v_{mn}\eta_\text{mn}\right\}, \quad (13)$$

where $\varsigma_\text{mn}=g_{nn}^m+2\Re\{\sum_{k\neq n}\sum_{l\neq n}v_{mk}g_{kl}^m v_{ml}\}$, g_{kl}^m is the element of $\mathbf{G}_\text{m}$ at the k-th row and l-th column and $\eta_\text{mn}=\sum_{j\neq n}g_{nj}^m v_{mj}$.

As it is described in [9], [21], the local optimal solution of the analog beamformer is

$$v_{mn} \quad =\begin{cases}1, & \eta_{mn}=0\\ \frac{\eta_{mn}}{|\eta_{mn}|}, & \eta_{mn}\neq 0\end{cases} \quad (14)$$

The final analog precoder algorithm lies in a convergent algorithm to find the local optimal solution for the analog precoder matrix, which is described in Algorithm1 [12]. First, start with an initial analog precoder which satisfies $|v_{\text{RF}}(i,j)|=1$. Then update $v_{\text{RF}}(i,j)$ at each iteration. The convergence of the local optimal solution is guaranteed.

For the partially connected structure, the analog precoder

Algorithm 1 Analog Precoder for hybrid SU-MIMO

1: Set $\mathbf{V}_{\text{RF}}=\mathbf{1}_{N_\text{t}\times N_{\text{RF}}}$ (We can also set this to any initiate value which satisfies $v_{\text{RF}}(i,j)=1$);
2: **for** $i=1:N_{\text{RF}}$ **do**
3: Construct $\mathbf{G}_m$ as defined in the above Equation 12;
4: Find $v_{\text{RF}}(i,j)=\psi(\sum_{m\neq j}g_{jm}^i v_{im})$;
5: If $w=0$,$\psi(w)=1$, otherwise, $\psi(w)=\frac{w}{|w|}$;
6: **end for**
7: Check the convergence. If not, go to Step 2.

$\mathbf{V}_{\text{RF}}$ is a block diagonal matrix, which can be denoted as

$$\mathbf{V}_{\text{RF}}=\begin{bmatrix}\mathbf{V}_1 & \mathbf{0} & \cdots & \mathbf{0}\\ \mathbf{0} & \mathbf{V}_2 & \cdots & \mathbf{0}\\ \mathbf{0} & \mathbf{0} & \ddots & \mathbf{0}\\ \mathbf{0} & \mathbf{0} & \cdots & \mathbf{V}_{N_{\text{RF}}}\end{bmatrix}. \quad (15)$$

For the analog precoder design for partially connected structure, we only need to update the nonzero elements of the analog precoder matrix.

As shown in [9], the 3-bit resolution phase shifters are sufficient to approach the performance of the infinite resolution phase shifters. For the hybrid beamforming structure with finite resolution phase shifters, we can first get the optimal analog precoder matrix, and then do the quantization for the nonzero elements of this matrix.

B. Design of Digital Precoder and Combiner

With the derived analog precoder, the effective channel at k-th subcarrier can be described as $\mathbf{H}_{\text{eff}}[k]=\mathbf{H}[k]\mathbf{V}_{\text{RF}}$. Then the digital precoder and combiner design problem is reduced to the solutions of the fully digital system with total power constraint, where the gNB is equipped with N_{RF} RF chains, $N_\text{t}=N_{\text{RF}}$ transmit antennas, and the UE is equipped with N_r receive antennas, and N_r RF chains.

The aim of the digital precoding design is a unitary precoding matrix which maximizes the achievable data rate and satisfies the total power constraint. Let $\mathbf{T}[k]$ be the unconstrained SVD digital precoder at subcarrier k and coefficient γ be the power constraint at the gNB. We perform SVD for the effective channel $\mathbf{H}_{\text{eff}}[k]=\mathbf{U}\mathbf{\Sigma}\mathbf{V}^H$, then precoder $\mathbf{T}[k]=\mathbf{V}$. Under total power constraint, the digital precoder is $\mathbf{V}_{\text{dig}}[k]=\gamma\mathbf{T}[k]=\gamma\mathbf{V}$ and the power constraint factor γ is given by

$$\gamma=\sqrt{\frac{P}{\sum_{k=1}^{K}\text{Tr}(\mathbf{V}_{\text{RF}}\mathbf{V}_{\text{dig}}[k]\mathbf{V}_{\text{dig}}^H[k]\mathbf{V}_{\text{RF}}^H)}}, \quad (16)$$

where P is the total power constraint at the gNB. Finally, the SVD digital combiner is given by $\mathbf{W}_{\text{digSVD}}[k]=1/\gamma\mathbf{U}$. In scenarios with ZF precoder, the digital precoder $\mathbf{V}_{\text{digZF}}$ and combiner $\mathbf{W}_{\text{digZF}}$ can be obtained:

$$\mathbf{V}_{\text{digZF}}=\gamma\mathbf{H}_{\text{eff}}^H[k]\left(\mathbf{H}_{\text{eff}}[k]\mathbf{H}_{\text{eff}}^H[k]\right)^{-1}, \quad (17)$$

$$\mathbf{W}_{\text{digZF}}=\mathbf{I}_{N_\text{r}}\frac{1}{\gamma}. \quad (18)$$

The detection is based the reduced complexity maximum-likelihood LLR metrics, developed by [19].In order to reduce the complexity of the algorithm, the precoder and combiner can be computed on a subband basis. The CSI remains constant for a group of subcarriers inside a coherence bandwidth. In this paper, the size of one subband is 12 subcarriers. The CSI is then averaged inside the subband, and the hybrid beamforming matrix is generated based on the average CSI to reduce the latency. Potentially, the size of subband can be increased as long as it remains inside the coherence bandwidth.

IV. Simulation Results

In this section, we evaluate hybrid and digital precoding algorithms for 5G NR Massive MIMO systems in single user scenario in terms of BLER and throughput. The comparison is provided for digital precoding and hybrid structures with fully and partially connected phase shifters. The effect of the phase shifters's resolution is also discussed. The algorithms are implemented and experiments are done in 5G NR simulator developed by TCL. The results thus provide an estimation of the performance levels in real-world 5G NR networks.

A. Simulation Assumptions

For our experiments, we have selected single-user downlink transmission with Modulation and Coding scheme 10. The downlink resources were allocated in 24 Radio Blocks. 5G NR supports various numerologies to adapt transmission to various carrier frequency, phase noise and Doppler by adjusting minimum subcarrier spacing. Although Massive MIMO in mmWave bands requires complex channel models that take into account the antenna geometry, we first validate our algorithms in frequency-flat Extended Pedestrian channel (EPA) model using numerology 0 (15 kHz subcarrier spacing) and carrier frequency at 2 GHz. We further extend our experiments towards the CDL-A channel with angle scaling and transmission using numerology 3 (120 kHz subcarrier spacing) and 26 GHz carrier frequency.

To avoid biased results, Monte-Carlo simulations were performed over 500 channel realizations. Throughput and BLER were selected as performance metrics. No retransmission protocols were considered. In all experiments the UE is equipped with four receive antennas and expects four data streams belonging to the same codeword (single-user spatial multiplexing transmission). If one layer is in outage, the full package is lost. The detection is based on reduced complexity maximum-likelihood LLR metrics, developed by [19]. In scenarios with SVD beamforming, the detection is preceded by the SVD combining matrix. In every experiment, hybrid algorithms are compared to the fully digital SVD precoding. Simulation parameters are summarized in Table 1.

TABLE I
Simulation parameters

Carrier Frequency	2 GHz, 26 GHz
Bandwidth	34.56 MHz (24 PRBs)
Numerology	3 (for CDL-A), 0 (for EPA)
PRB size	12 subcarriers
Subband size	12 subcarriers
Modulation	16 QAM
Coding	LDPC coding
Antenna Array	UL isotropic antenna elements
Channel Model	CDL-A, EPA
Number of tx antennas N_{t}	$\{4, 8, 16, 64\}$
Number of rx antennas N_{r}	4
Number of RF chains	$\{4, 8, 16\}$

B. CDL Channel model with Angle Scaling

The propagation environment of large-scale MIMO systems is modeled as CDL-A channel with angle scaling [16]. This model represents a single realization of the 5G channel due to the predefined angle value for each CDL channel model. The precoder statistics thus might be biased, and a fixed precoder may perform better than open-loop, closed-loop or reciprocity beamforming. Angle scaling allows an adequate application of CDL model in massive MIMO systems with beamforming. The angle scaling is described as following [22]:

$$\phi_{n,\text{scaled}} = \frac{\text{AS}_{\text{desired}}}{\text{AS}_{\text{model}}}(\phi_{n,\text{model}} - \mu_{\phi,\text{model}}) + \mu_{\phi,\text{desired}} \qquad (19)$$

where $\phi_{n,\text{model}}$ is the tabulated CDL angle, AS_{model} is the rms angular spread of the tabulated CDL, $\mu_{\phi,\text{model}}$ is the mean angle of the tabulated CDL, $\mu_{\phi,\text{desired}}$ is the desired mean angle, $\text{AS}_{\text{desired}}$ is the desired rms angular spread, $\phi_{n,\text{scaled}}$ is the resulting scaled cluster angle.

For the above formula, ratio $\frac{\text{AS}_{\text{desired}}}{\text{AS}_{\text{model}}} = 1$ and $\mu_{\phi,\text{model}}$ is the weighted average value:

$$\mu_{\phi,\text{model}} = angle\left(\sum P_{n,\text{model}} \exp(j\phi_{n,\text{model}})\right), \qquad (20)$$

where $P_{n,\text{model}}$ denotes power of n-th cluster). The weighted average value $\mu_{\phi,\text{desired}}$ yields the random value: uniformly distributed within $[-60, 60]$ degrees for azimuth angle spread of departure (AoD), within $[90, 135]$ degrees for zenith angle spread of departure (ZoD), within $[-180, 180]$ degrees for azimuth angle spread of arrival (AoA), within $[45, 90]$ degrees for zenith angle spread of arrival (ZoA).

In our simulations, We use the uniform planar arrays (ULAs).

C. Numerical results

In the first experiment, we analyzed the performance of the baseline SVD digital precoding and various hybrid beamforming methods. The gNB is equipped with $N_{\text{RF}} = 4$ RF chains and $N_{\text{t}} = 16$ antennas serves a single user with $N_{\text{r}} = 4$ antennas. We begin the experiment with flat-fading EPA channel to validate our algorithms (see Fig.3). For numerology 0 and MCS 10, the throughput is limited by 14 Mbps. The digital SVD precoding expectedly shows the best result, followed by fully connected hybrid beamforming. In the low SNR regime, hybrid SVD (purple plot) takes over hybrid ZF (green plot),

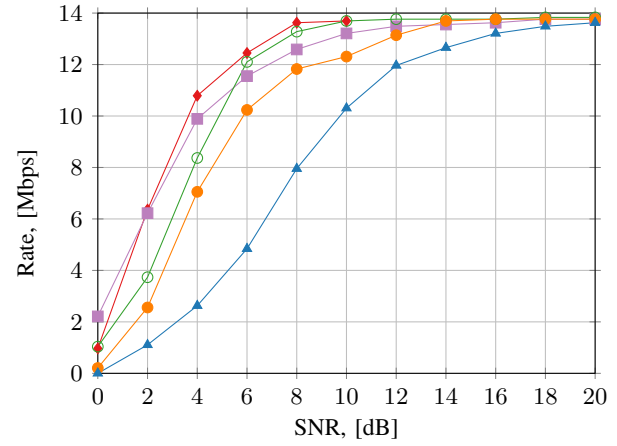

(a) Throughput

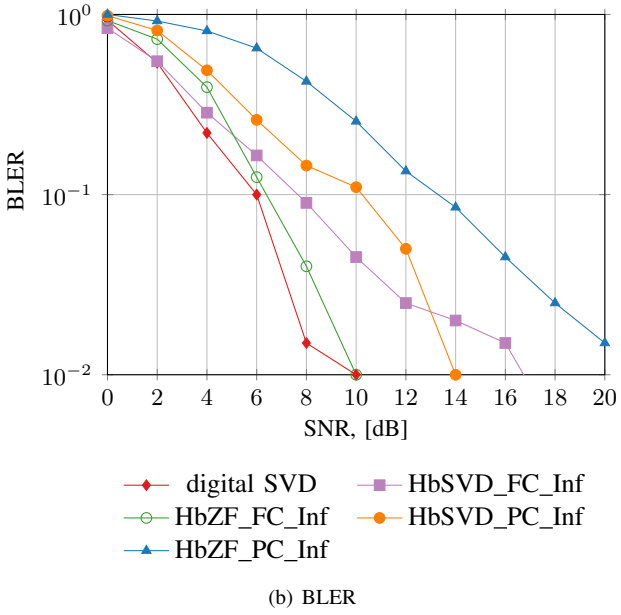

(b) BLER

Fig. 3. Throughput (top) and BLER (bottom) for the EPA scenarios with MCS 10 and 24 PRBs for hybrid structures with infinite resolution of phase shifters and 16 transmit antennas. Numerology is 0. Here, "HbSVD_FC_Inf" denotes hybrid SVD precoding with fully connected phase shifters. Following the same logic, "HbZF_FC_Inf" stands for hybrid ZF with fully connected phase shifters, while "HbSVD_PC_Inf" and "HbZF_PC_Inf" – partially connected structures with SVD and ZF precoding respectively.

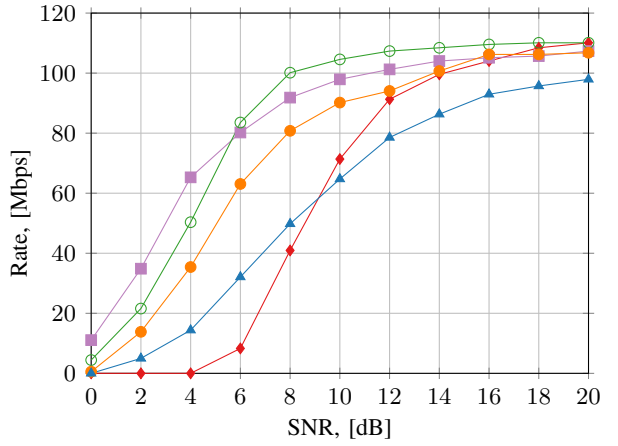

(a) Throughput

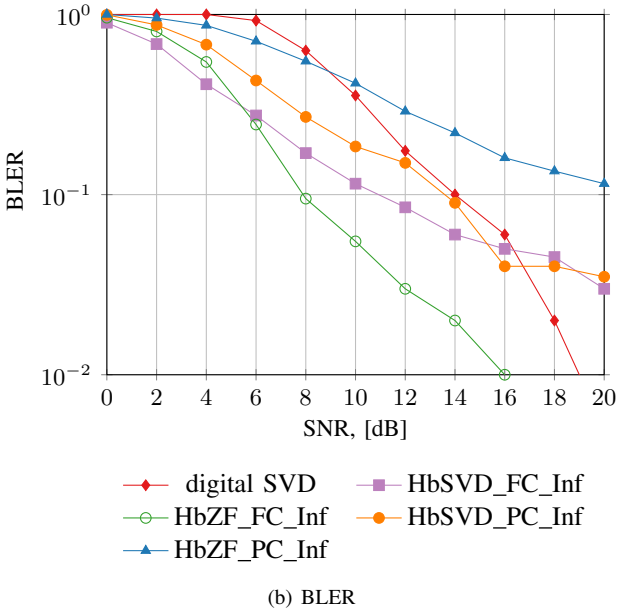

(b) BLER

Fig. 4. Throughput (top) and BLER (bottom)for the CDL-A scenarios with MCS 10 and 24 PRBs for hybrid structures with infinite resolution of phase shifters. Numerology is 3. Here, "HbSVD_FC_Inf" denotes hybrid SVD precoding with fully connected phase shifters. Following the same logic, "HbZF_FC_Inf" stands for hybrid ZF with fully connected phase shifters, while "HbSVD_PC_Inf" and "HbZF_PC_Inf" – partially connected structures with SVD and ZF precoding respectively.

while at high SNR hybrid ZF slightly outperforms hybrid SVD scheme, till they both reach maximum throughput. However, among partially connected strictures, the SVD (orange curve) has a strong advantage over the ZF (blue curve), which grows with the increase of SNR.

The principal difference between the performance in EPA and CDL-A channel (Fig.4) lies in the performance of the digital SVD precoder: in CDL channel the digital SVD scheme performs worse than the hybrid beamforming. This is due to the fact that in highly selective frequency channels, such as CDL, certain eigenvalues of the channel matrix might be significantly lower (or higher) compared to other eigenvalues, and some spatial layers can thus experience an outage event, causing a failure of the full codeword. Note that compared to the EPA channel with numerology 0, the maximum throughput in CDL channel with numerology 3 scales with the factor 2^{ν}, where ν is numerology, and thus achieves 112 Mbps.

The second experiment studies the influence of the phase shifters's resolution on the performance of our hybrid SVD algorithm in CDL channel. In practical hybrid massive MIMO system, only finite resolution phase shifters are available. In this experiment, we successively consider one, two, and three bits of resolution (see Fig.5). While difference between infinite, three and two bit resolution is almost negligible, phase shifters with a single bit resolution introduce two dB of performance loss.

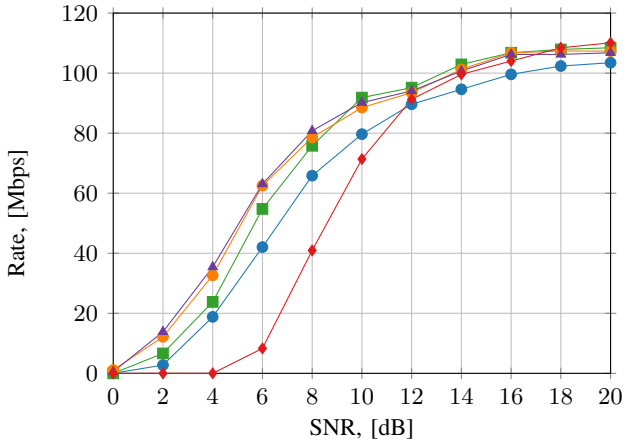

(a) Throughput

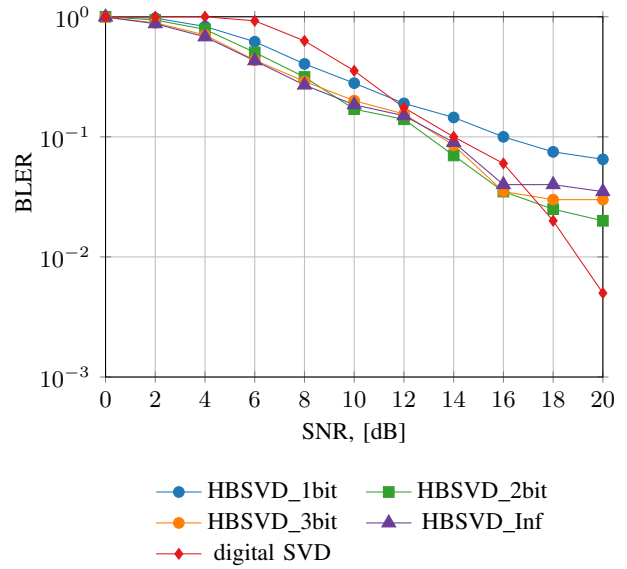

(b) BLER

Fig. 5. Throughput (top) and BLER (bottom) for hybrid SVD system with different resolutions of phase shifters: one, two, three bits and infinite resolution. The transmission is performed using MCS 10 and 24 PRBs in CDL-A channel model with angle scaling

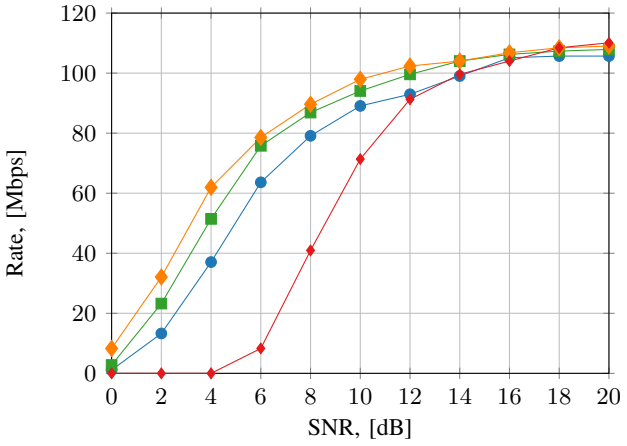

(a) Throughput

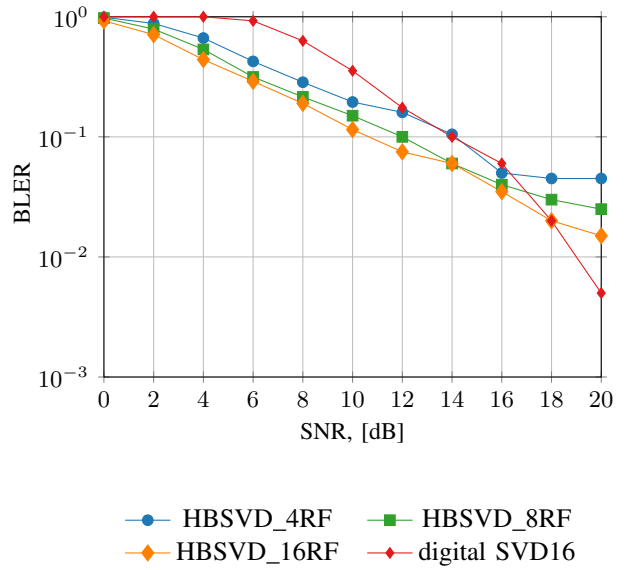

(b) BLER

Fig. 6. Throughput (top) and BLER (bottom) for hybrid SVD precoding with different number of RF chains $N_{\text{RF}} \in \{4, 8, 16\}$. The transmission is performed using MCS 10 and 24 PRBs in CDL-A channel model with angle scaling. Number of transmit antennas N_{t} is 16 and does not vary in this experiment.

The third experiment investigates the influence of the number of RF chains on our hybrid SVD beamforming algorithm. In this experiment, the gNB is equipped with 16 transmit antennas, and the number of RF chains varies between four and sixteen. As it is shown in Fig.6, the overall throughput and BLER improves with the increase of the number of RF chains, however, it is not reasonable to deploy RF chains that exceed number of data streams more than twice ($N_{\text{RF}} > 2N_{\text{s}}$), as it does not bring a noticeable gain.

In the last experiment, we evaluate the gain that is delivered by increased number of transmit antennas at the base station. Exceptionally, this experiment was done for CDL-A channel model and numerology 0 in the attempt to speed up computations. In the initial settings for this experiment, the base station deploys $N_{\text{RF}} = 4$ RF chains and $N_{\text{r}} = 4$ receive antennas. The beamforming scheme is hybrid SVD with partially connected phase shifters with four bit resolution. Number of transmit antennas then gradually increases: $N_{\text{t}} \in \{4,\ 8,\ 16,\ 64\}$. As it can be seen from Fig.7, the performance improves without saturation with the increase of the ratio $\frac{N_{\text{t}}}{N_{\text{RF}}}$.

V. Conclusion

We experimentally quantified performance of the dual-stage hybrid SVD and ZF beamforming algorithms in MATLAB 5G NR simulator. Our algorithms apply total power constraint. Digital SVD beamforming scheme, although not practically feasible, was taken as a baseline for a comparison. The experiments were performed for frequency-flat EPA channel, and for complex frequency-selective CDL model, which takes

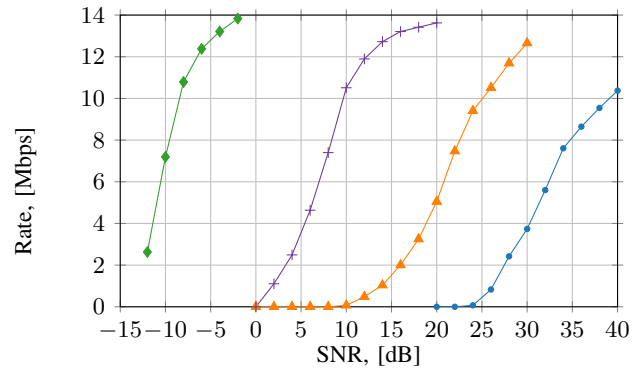

(a) Throughput

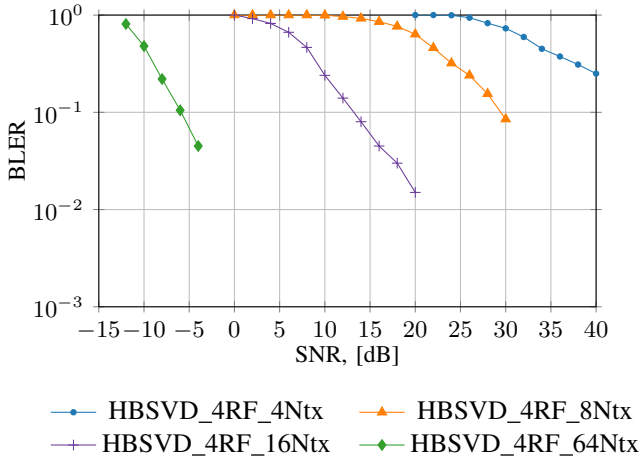

(b) BLER

Fig. 7. BLER and throughput for SVD hybrid beamforming with $N_t \in \{4, 8, 16, 64\}$ and four RF chains. Exceptionally, for this scenario CDL-A channel model with angle scaling was taken with numerology 0 transmission.

into account antenna geometry. Millimeter wave propagation was addressed with CDL channel at 26GHz frequency. During this study, we observed a limitation of the SVD algorithms in frequency-selective channels due to some eigenvalues of the channel matrix being too small or too big. Based on the results of the experiments with fully and partially connected hybrid structures, we concluded that two bits resolution phase shifters provide results approaching phase shifters with infinite resolution. Varying number of RF chains while keeping constant number of transmit antennas, we experimentally proved that increasing N_{RF} more than twice N_s does not contribute to the performance.

We are currently working on hybrid beamforming for multi-user MIMO as well as integration of the quantized precoder feedback, defined in the standard. Future work will evaluate the loss (if any) caused by the knowledge of quantized precoder instead of full CSI, which was assumed in this paper.

VI. Acknowledgement

The work presented in this paper is partially supported by the project French FUI MASS-START (mass-start.fr).

References

[1] T. L. Marzetta, "Massive mimo: An introduction," *Bell Labs Technical Journal*, 2015.

[2] T. S. Rappaport, S. Sun, R. Mayzus, H. Zhao, Y. Azar, K. Wang, G. N. Wong, J. K. Schulz, M. Samimi, and F. Gutierrez, "Millimeter wave mobile communications for 5g cellular: It will work!" *IEEE Access*, 2013.

[3] Z. Pi and F. Khan, "An introduction to millimeter-wave mobile broadband systems," *IEEE Communications Magazine*, June 2011.

[4] S. A. Busari, S. Mumtaz, S. Al-Rubaye, and J. Rodriguez, "5G Millimeter-Wave Mobile Broadband: Performance and Challenges," *IEEE Communications Magazine*, June 2018.

[5] Ericsson, "R1-1612351, Type II CSI Feedback," *3GPP TSG RAN WG1 Meeting#87, Reno, USA*, November 2016.

[6] X. Zhang, A. F. Molisch, and S.-Y. Kung, "Variable-phase-shift-based RF-baseband codesign for MIMO antenna selection," *IEEE Transactions on Signal Processing*, Nov 2005.

[7] T. L. Marzetta, E. G. Larsson, H. Yang, and H. Q. Ngo, *Fundamentals of Massive MIMO*. Cambridge University Press, 2016.

[8] S. S. Christensen, R. Agarwal, E. D. Carvalho, and J. M. Cioffi, "Weighted sum-rate maximization using weighted MMSE for MIMO-BC beamforming design," *IEEE Transactions on Wireless Communications*, December 2008.

[9] F. Sohrabi and W. Yu, "Hybrid digital and analog beamforming design for large-scale antenna arrays," *IEEE Journal of Selected Topics in Signal Processing*, April 2016.

[10] O. E. Ayach, S. Rajagopal, S. Abu-Surra, Z. Pi, and R. W. Heath, "Spatially Sparse Precoding in Millimeter Wave MIMO Systems," *IEEE Transactions on Wireless Communications*, March 2014.

[11] D. C. Arajo, E. Karipidis, A. L. F. de Almeida, and J. C. M. Mota, "Hybrid beamforming design with finite-resolution phase-shifters for frequency selective massive MIMO channels," in *2017 IEEE International Conference on Acoustics, Speech and Signal Processing (ICASSP)*, March 2017, pp. 6498–6502.

[12] F. Sohrabi and W. Yu, "Hybrid analog and digital beamforming for mmwave OFDM large-scale antenna arrays," *IEEE Journal on Selected Areas in Communications*, July 2017.

[13] S. Payami, M. Ghoraishi, M. Dianati, and M. Sellathurai, "Hybrid beamforming with a reduced number of phase shifters for Massive MIMO systems," *IEEE Transactions on Vehicular Technology*, June 2018.

[14] D. H. N. Nguyen, L. B. Le, T. Le-Ngoc, and R. W. Heath, "Hybrid MMSE precoding and combining designs for mmwave Multiuser systems," *IEEE Access*, vol. 5, pp. 19 167–19 181, 2017.

[15] R. Mndez-Rial, C. Rusu, N. Gonzlez-Prelcic, A. Alkhateeb, and R. W. Heath, "Hybrid MIMO architectures for millimeter wave communications: Phase shifters or switches?" *IEEE Access*, 2016.

[16] 3GPP, "Study on channel model for frequency spectrum above 6 GHz," *Technical Report TR 38.900 V14.2.0 Release 14*, June 2017.

[17] E. Bjrnson, E. G. Larsson, and T. L. Marzetta, "Massive MIMO: ten myths and one critical question," *IEEE Communications Magazine*, Feb. 2016.

[18] M. Costa, "Writing on dirty paper (corresp.)," *IEEE Transactions on Information Theory*, vol. 29, no. 3, pp. 439–441, May 1983.

[19] R. Ghaffar and R. Knopp, "Low Complexity Metrics for BICM SISO and MIMO systems," in *Vehicular Technology Conference (VTC 2010-Spring), 2010 IEEE 71st*, May 2010, pp. 1–6.

[20] X. Jiang and F. Kaltenberger, "Channel reciprocity calibration in TDD hybrid beamforming massive MIMO systems," *IEEE Journal of Selected Topics in Signal Processing, Vol PP, N99, 23 March 2018*, 03 2018. [Online]. Available: http://www.eurecom.fr/publication/5298

[21] Z. Pi, "Optimal transmitter beamforming with per-antenna power constraints," in *2012 IEEE International Conference on Communications (ICC)*, June 2012.

[22] 3GPP, "Summary of email discussion [87-30] on NR-MIMO calibration," *3GPP TSG RAN WG1 MeetingNR AH: Discussion and Decision*, January 2017.